

The Control of Satellites with Microgravity Constraints:
The COMET Control System

Walter Grossman
Madison Guidance, Navigation & Control
616 Madison Court
Yorktown Heights, NY 10598-3722
e-mail: w.grossman@ieee.org

Douglas Freesland
CTA Space System
1521 Westbranch Drive
McLean, VA 22102-3201

I. Nomenclature

- \hat{b} - Unit vector in direction of local magnetic field.
- g_p - Proportional control gain.
- g_d - Derivative control gain.
- g_i - Integral control gain.
- g_w - Wheel speed control feedback gain.
- G - Gravity gradient torque.
- h - Spacecraft internal angular momentum.
- J - Spacecraft inertia matrix.
- \hat{n} - Momentum management axis. Unit vector along intersection of magnetic control subspace and wheel control subspace.
- n_{\perp} - \mathcal{R}^2 space perpendicular to \hat{n} .
- q - Attitude quaternion.
- R_i - Saturation ratio of i th actuator. $R_i = |\tau_i|/\tau_{max\ i}$.
- v - Linear control of dynamics-inverted system.
- w - Wheel speed vector $[0 \ w_y \ w_z]'$.
- w_y, w_z - y and z momentum wheel speeds, respectively.
- \hat{x} - Unit vector along spacecraft x -axis.
- ϵ_p - Euler axis attitude error derived from ϵ_q . $\epsilon_p = 2\epsilon_q(0)[\epsilon_q(1) \ \epsilon_q(2) \ \epsilon_q(3)]'$.
- ϵ_q - Quaternion error. $\epsilon_q = q \otimes q_{ref}^{-1}$.
- ϵ_w - Wheel speed error. $\epsilon_w = w - w_{ref}$.
- ϵ_{ω} - Spacecraft angular velocity error. $\epsilon_{\omega} = \omega - \omega_{ref}$.
- τ - Spacecraft control torque.
- τ_1 - Attitude control torque projected onto \hat{n} .
- τ_2 - Attitude control torque projected onto n_{\perp} .
- τ_i - Actuation command for i th actuator.
- $\tau_{max\ i}$ - Saturation value of i th actuator.
- τ_{m1} - Attitude control torque projected onto n_{\perp} effectuated by magnetic torquers.

- τ_{m2} - Momentum management torque parallel to \hat{n} effectuated by magnetic dipole torquers.
- τ_{w1} - Attitude control torque projected onto n_{\perp} effected by momentum wheel actuators.
- τ_{w2} - Momentum management control torque parallel to \hat{n} effectuated by momentum wheels.
- ω - Spacecraft angular velocity.
- \otimes - Quaternion multiplication operator.

II. Introduction

The COMmercial Experimental Transporter (COMET) satellite provides a microgravity environment for experimental payloads. For the first thirty days of the mission the satellite is operated in a solar-inertial fixed attitude to maximize the power profile. The spacecraft is then pointed along the velocity vector and the experiment carrier is released for deboosting and recovery. The spacecraft is then nadir pointed and additional microgravity experiments are conducted.

The COMET Attitude Determination and Control System (ADACS) supports these mission requirements by combining inverse dynamics nonlinear feedback with a novel momentum management technique.

Inverse dynamics was developed in the middle 1980's for multi-mission, multi-configuration aircraft [1, 2] and subsequently applied to spacecraft [3].

The technique uses nonlinear feedback to globally transform nonlinear system dynamics into a linear system described by a linear second-order differential equation. Since the transfor-

mation is global and exact only a single set of control gains is required for both small-angle attitude maintenance and large-angle attitude maneuvers. The technique inherently accommodates multiple spacecraft mass configurations without the need for multiple sets of control gains. The inverse dynamics technique compensates for and exploits spacecraft precession to achieve three-axis attitude control using two reaction wheels.

The COMET momentum management system controls reaction wheel speed while preserving the satellite microgravity environment. Unlike the inner-loop/outer-loop structure common to most satellites, the COMET momentum management system calculates the momentum management torques as an integral part of the attitude control torque.

III. Inverse Dynamics Control

The spacecraft dynamics are written

$$J(q)\dot{\omega} + \underbrace{\omega^\times [J(q)\omega + h]}_{\text{precession}} + \underbrace{G(q)}_{\text{grav grad}} = \tau. \quad (1)$$

The plant dynamics described by (1) are inverted and *globally* linearized

$$\tau = J(q)v + \omega^\times [J(q)\omega + h] + G(q) \quad (2)$$

$$v = -g_p \epsilon_q - g_d \epsilon_\omega - g_i \int_0^t \epsilon_q(\lambda) d\lambda. \quad (3)$$

Substituting equations (2) and (3) into (1) yields the linear differential equation

$$\dot{\omega} = -g_p \epsilon_q - g_d \epsilon_\omega - g_i \int_0^t \epsilon_q(\lambda) d\lambda. \quad (4)$$

The feedback gains, g_p , g_d , and g_i are chosen using LQR design methods.

Implementation of the inverse dynamics control law described by equations (2) and (3), requires full-state feedback of spacecraft attitude and angular velocity. Many spacecraft lack the inertial measurement unit (IMU) necessary to measure angular rates. COMET has an IMU but its use is necessarily limited to conserve power.

It was shown [4, 5] that inverse dynamics can be robustly implemented with only partial-state

feedback using a Kalman observer to estimate the unmeasured velocity state. Including the position and velocity estimates from the Kalman observer, the control law described by equations (2) and (3) is modified

$$\tau = J(\hat{q})v + \hat{\omega}^\times [J(\hat{q})\hat{\omega} + h] + G(\hat{q}) \quad (5)$$

$$v = -g_p \hat{\epsilon}_q - g_d \hat{\epsilon}_\omega - g_i \int_0^t \hat{\epsilon}_q(\lambda) d\lambda, \quad (6)$$

where the $\hat{\cdot}$ indicates the observer-estimated value.

The torque vector derived from the control law, equations (5) and (6), is applied to the COMET microgravity attitude actuators.

IV. Torque Distribution & Momentum Management

A. The Actuator Suite

The COMET microgravity actuator suite consists of three 100 $a\text{-m}^2$ electromagnetic torque coils along the spacecraft x , y , and z body axes and two 2 newton-meter-second momentum wheels along the spacecraft y and z body axes. There is no momentum wheel parallel to the spacecraft x -axis. (COMET is equipped with six 44 newton (10 lb) cold gas thrusters. They impart accelerations which exceed microgravity limits so their use is restricted to initial acquisition and recovery system reaction control.)

At the nominal 250 nautical mile altitude the magnetic torques deliver approximately 1×10^{-3} newton-meter torque in the plane perpendicular to the local magnetic field. The momentum wheels deliver approximately 8.5×10^{-3} newton-meter torque.

B. Momentum Management by Torque Decomposition

Three wheel and four wheel momentum management schemes are usually implemented as a feedback outer-loop external to the attitude control system inner-loop controller. Gas jets provide instantaneous three-axis desaturation control authority. For non-equatorial orbits mag-

netic dipoles provide instantaneous two-axis desaturation and over-orbit three-axis momentum management.

Inner-loop/outer-loop control structure separation works with spacecraft having three or four wheels because the wheel axes span \mathcal{R}^3 . The attitude control torque is exactly decomposed onto the wheel axes and effectuated entirely with the momentum wheel actuators. The instantaneous momentum error is projected onto the magnetic control subspace \mathcal{R}^2 normal to the local external field and is removed. Over orbit the magnet control subspace spans \mathcal{R}^3 and wheel momentum is maintained. The control problem separates whereby high-bandwidth attitude control is effected by the momentum wheels and low-bandwidth momentum control is effect by the magnetic torque coils.

Having only two wheels, the COMET microgravity control system cannot be partitioned into this inner-loop/outer-loop structure. The COMET attitude control torque must be applied using a combination of the wheels and torque coils while momentum is simultaneously maintained over orbit. The momentum control torques are calculated continuously and as an integral part of the attitude control torques.

The wheel torque subspace spans \mathcal{R}^2 . When the spacecraft x -axis is not colinear with the local magnetic field the magnetic torque subspace spans a different \mathcal{R}^2 and the actuator torque space is overdetermined. The intersection of the two subspaces represents a direction in \mathcal{R}^3 where the attitude control torque can be applied *either using the magnetic torquers or the momentum wheels*. This axis is the "momentum management axis" where some portion of the momentum error can be removed without disturbing spacecraft attitude. See figure 1.

The COMET momentum management and attitude control torque distribution technique is captured mathematically by solving a system of linear constraints. The decomposition steps are summarized:

$$\hat{n} = \frac{\hat{x} \times \hat{b}}{|\hat{x} \times \hat{b}|} \quad (7)$$

$$\tau_1 = \hat{n}' \tau \quad (8)$$

$$\tau_2 = (I - \hat{n}\hat{n}') \tau \quad (9)$$

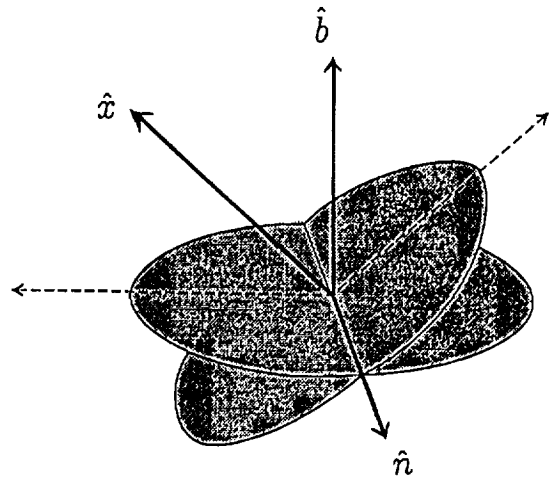


Figure 1: The "torque space" and the momentum management axis.

$$\begin{pmatrix} 0 \\ 0 \\ \tau_2 \\ 0 \\ 0 \end{pmatrix} = \begin{pmatrix} \hat{b}' & 0 \\ 0 & \hat{x}' \\ I - \hat{b}\hat{b}' & I - \hat{x}\hat{x}' \\ \hat{n}' & 0 \\ 0 & \hat{n}' \end{pmatrix} \begin{pmatrix} \tau_{m1} \\ \tau_{w1} \end{pmatrix} \quad (10)$$

$$\tau_1 = (\hat{n}' \quad \hat{n}') \begin{pmatrix} \tau_{m1} \\ \tau_{w1} \end{pmatrix} \quad (11)$$

Equation (10) represents the constraints for solving for the torque in subspace n_{\perp} . These constraints are:

1. Zero magnetic torque in direction of \hat{b} .
2. Zero wheel torque in direction of \hat{x} .
3. The sum of the wheel and magnetic torque in their respective subspaces equals the component of the attitude control torque in space n_{\perp} .
4. Zero magnetic torque in direction of \hat{n} .
5. Zero wheel torque in direction of \hat{n} .

The 7×6 matrix in (10) is a rank 6 matrix and the equation has a unique solution. (In COMET these equations are solved using the numerically robust QR decomposition.) Equation (11) is underdetermined. *Any combination of magnetic and wheel torque in the direction \hat{n} which equals τ_1 will correctly maintain the spacecraft attitude.*

The momentum management torque is proportional to the wheel speed error projected onto \hat{n} . A wheel speed corrective torque and

a compensating magnetic torque are applied in the \hat{n} and $-\hat{n}$ direction, respectively.

$$\tau_{w2} = -g_w \hat{n} \hat{n}' \epsilon_w \quad (12)$$

$$\tau_{m2} = \tau_1 - \tau_{w2}. \quad (13)$$

The final actuator torques are the sum of the components in the \hat{n} and n_{\perp} spaces

$$\tau_w = \tau_{w1} + \tau_{w2} \quad (14)$$

$$\tau_m = \tau_{m1} + \tau_{m2}. \quad (15)$$

C. Saturation Control

The computed wheel torques and magnetic dipole moments may drive the actuators into saturation. Saturation does not usually occur uniformly across all the actuators. The effect of saturation is to misdirect the corrective rotation of the satellite.

Saturation control in COMET is based upon the heuristic that it is preferable to maintain the *direction* of the control torque at reduced magnitude than to apply maximum control authority in the wrong direction.

The five actuator commands (two wheel torques, three magnetic dipole values) are calculated and five saturation ratios $R_i = |\tau_i|/\tau_{max i}$ are calculated. If any of these five ratios exceeds unity then *all* the actuator commands are scaled by the largest of these five ratios.

The effect of occasional actuator saturation upon linear systems is generally benign and not destabilizing. The effect of actuator saturation upon an inverse dynamics control system is complicated in that saturation leads to incomplete inversion. Simulation has demonstrated good system performance even with occasional saturation. The effect of saturation on incomplete dynamics inversion and control system performance is an area which requires future research.

V. Simulation

Simulations demonstrate the performance of the COMET microgravity control system.

Gravity gradient and aerodynamic torques are the dominant disturbances and are simulated. The simulation orbit is circular at 463 km (250 NM) altitude. The F10.7 solar flux level is 116.

Spacecraft state estimates generated by attitude determination system are used for calculation the attitude and rate errors. Except where noted, the IMU is off and feedback linearization is achieved using angular velocity estimates.

Simulation series (1) demonstrates COMET solar-pointing performance with a momentum bias. The spacecraft attitude recovers from the initial 15° error. Momentum wheel rates converge to their nominal 1500 RPM bias levels.

Lack of sensor input combined with unmodelled aerodynamic torques cause the attitude error to increase in the umbra. This pointing error is due to attitude estimation error developed in the Kalman Filter extrapolation step. Simulation series (2) shows represents the same run as series (1) except the IMU is on and satellite body rates are directly measured. Umbra performance is greatly improved.

Simulation series (3) demonstrates COMET solar-pointing performance without momentum bias. The spacecraft attitude recovers from the initial error. Momentum wheel mean rates converge to zero. The attitude control system in series (3) is identical to that of series (1) demonstrating control system flexibility in accommodating different momentum configurations. This flexibility is a consequence of the exact *global* linearization provided by the inverse dynamics control law. With equal flexibility the control system accommodates spacecraft with varying mass properties. COMET is a multi-configuration spacecraft which uses the same control law for all its mass configurations.

Simulation series (4) demonstrates COMET Earth-pointing performance¹.

Simulation series (5) demonstrates the COMET large-slew microgravity transition

¹In Earth-pointing mode the COMET spacecraft coordinate system differs from the conventional local vertical system. In this mode the roll axis (x -axis) is nadir-pointing, the yaw axis (z -axis) is aligned anti-parallel to the orbit normal, and the pitch axis (y -axis) completes the triad, pointing approximately in the velocity direction.

from solar-pointing to Earth-pointing. Note the rate quenching of the COMET pitch momentum wheel (yaw wheel by conventional terminology). Spacecraft acceleration is maintained within the $10^{-5}g$ microgravity acceleration limit *during the slew*.

Simulation series (6) demonstrates COMET slewing 90° in pitch and yaw and holding to an arbitrary attitude. Momentum wheels maintain their 1500 RPM bias during the slew. This mode is used for reentry attitude control prior to recovery capsule deboosting.

Simulation series (7) demonstrates the synthesized roll control performed without a roll wheel. This synthesized roll is a consequence of the inclusion of the precession term in the inverse dynamics. Series (7a) shows the large roll when the precession term is not included. Simulation series (7b) shows the roll error reduction caused by inclusion of the precession term.

Simulations (1)-(7) demonstrate the performance of the COMET attitude control system. Slewing of the reaction wheel during transition and maintenance of their speeds in the steady-state demonstrates the performance of the novel COMET momentum management technique. Operational flexibility to the variety mass properties, momentum biases and command attitudes is a feature inherent to the method of inverse dynamics control.

From simulation experiments, inverse dynamics control is empirically known to be robust to large variations in the "model" plant. Simulation series (8) demonstrates that COMET is robust to large uncertainty to mass properties. In this simulation the three mass principle axes of the true satellite are skewed 15° from their "model" orientation. The system remains stable and within specification. The mass properties mismatch does causes a 50% increase RMS attitude error (see simulation series 1 for comparison.)

VI. Conclusion

The COMET attitude determination and control system, using inverse dynamics and a

novel torque distribution/momentum management technique, has shown great flexibility, performance, and robustness.

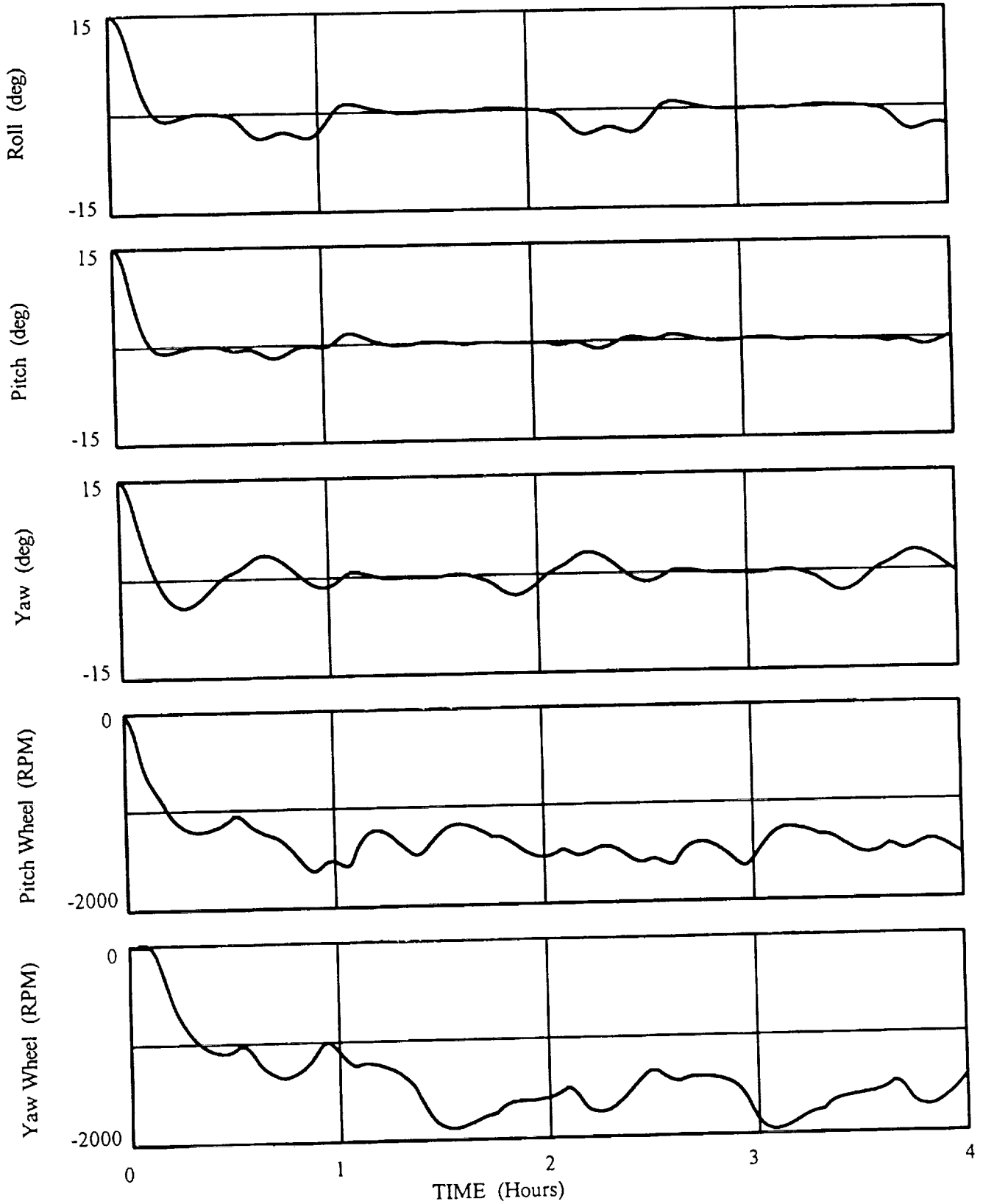
Three-axis control with two wheels is an inherent consequence of inverse dynamics control which allows for reduction in spacecraft weight and cost, or alternatively, provides a simple means of failure-redundancy for three-wheel spacecraft.

The control system, *without modification*, has continued to perform well in spite of large changes in spacecraft mass properties and mission orbit altitude that have occurred during development². This flexibility has obviated imposition of early stringent ADACS design constraints and has greatly reduced commonly incurred ADACS modification costs and delay associated with program maturation.

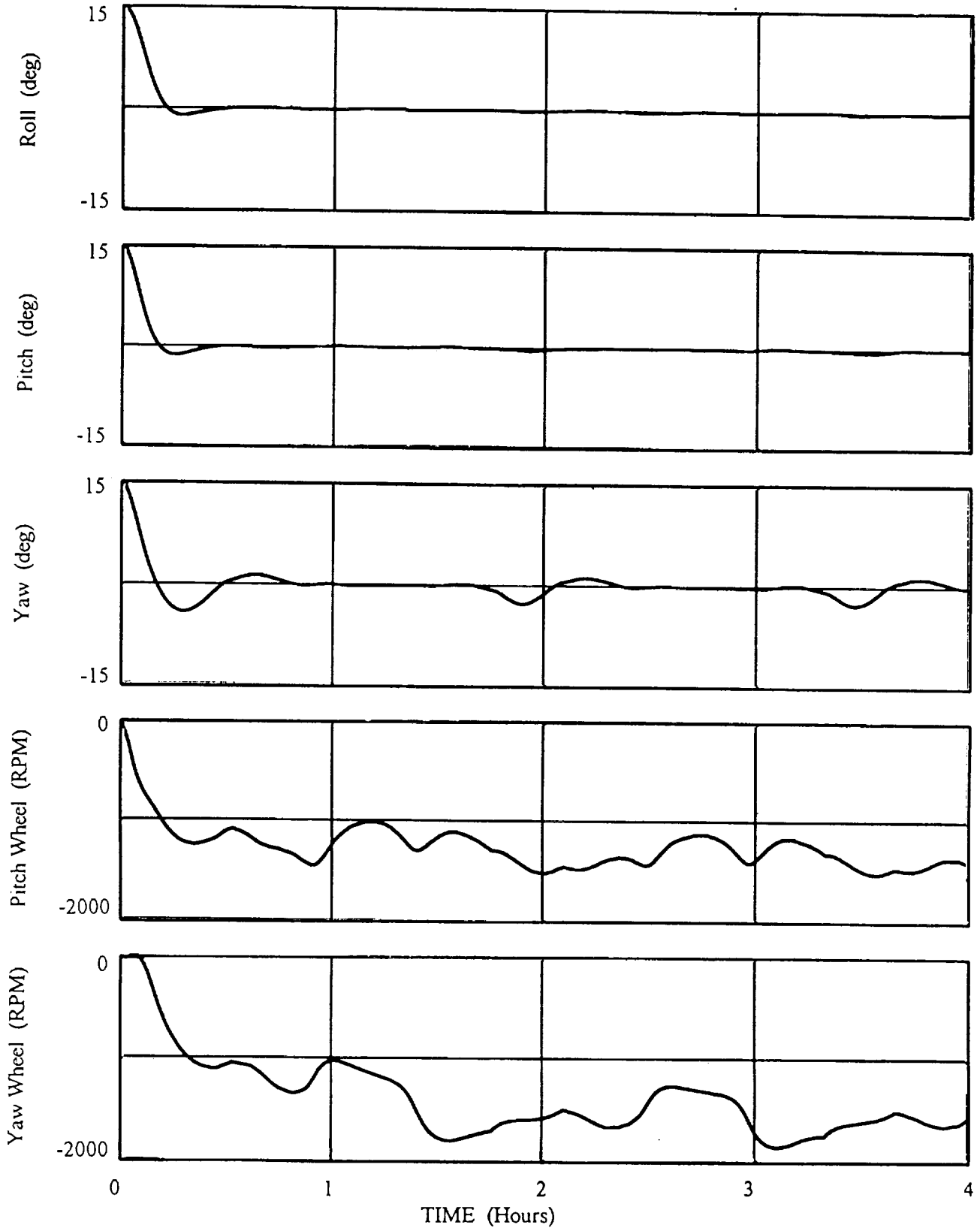
-
- [1] G. Meyer, R. Su, and L. R. Hunt, "Application of nonlinear transformations to automatic flight control," *Automatica*, vol. 20, no. 1, pp. 103-107, 1984.
 - [2] A. Isidori, "Nonlinear control systems," in *Lecture Notes in Control and Information (2nd edition)*, Springer-Verlag, 1989.
 - [3] T. A. W. Dwyer, "Exact nonlinear control of large angle rotational maneuvers," *IEEE Trans. Automatic Control*, vol. AC-29, no. 9, pp. 769-774, 1984.
 - [4] W. Grossman, F. Khorrami, and B. Friedland, "Observer-based design for robust control of robot manipulators," in *Proceedings of the 1990 American Control Conference*, (San Diego, California), pp. 731-736, May 1990.
 - [5] W. D. Grossman, *An Observer-based Design for Control of Nonlinear Systems and Applications to Robot Manipulators*. Degree of Engineer thesis, Polytechnic University, Brooklyn, New York, 1992.

²Increases in spacecraft mass has lead to reduction of orbit altitude from the original 556 km (300 nm) altitude to the 463 km (250 nm) altitude. The control system was designed for the original altitude.

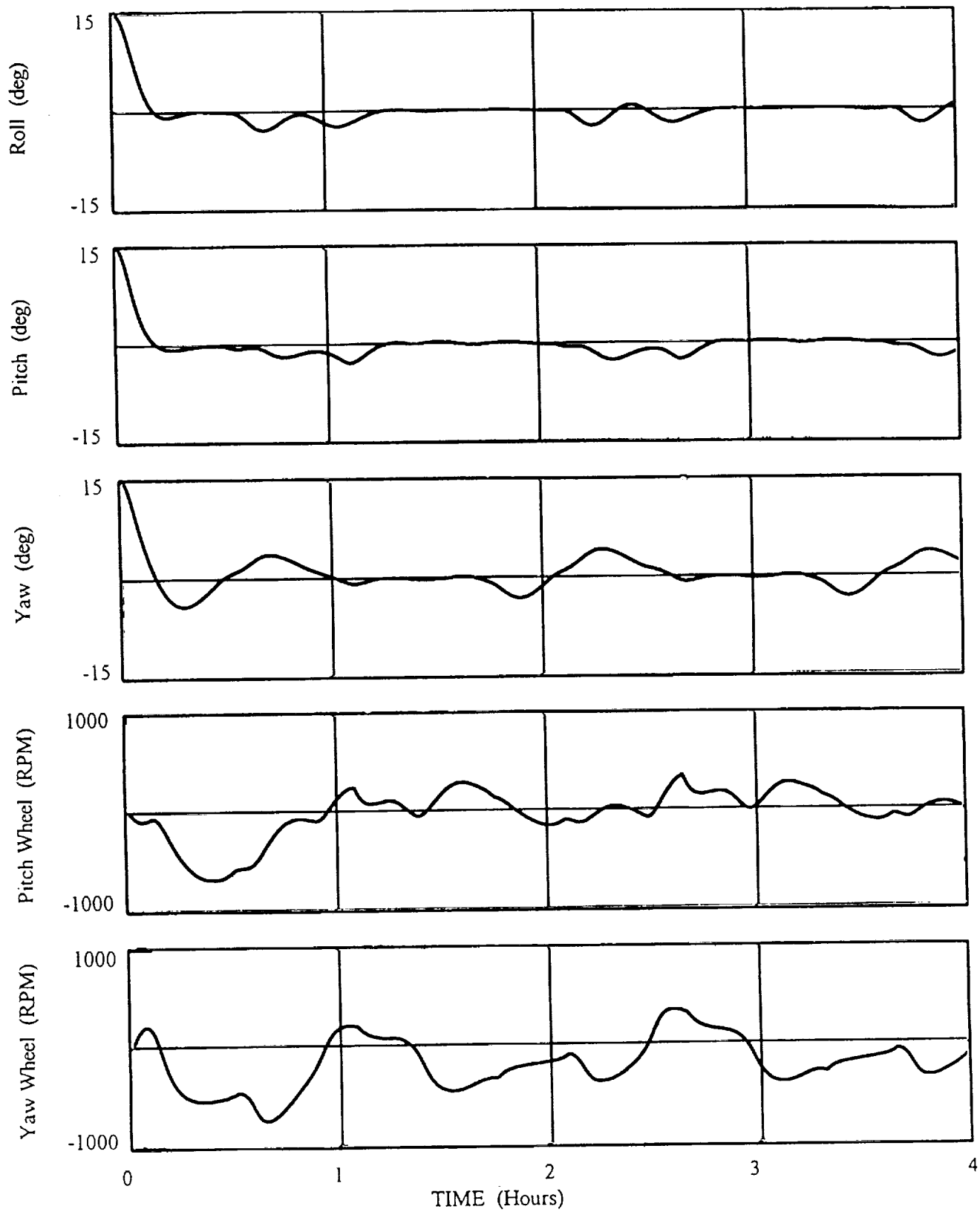
Simulation Series 1



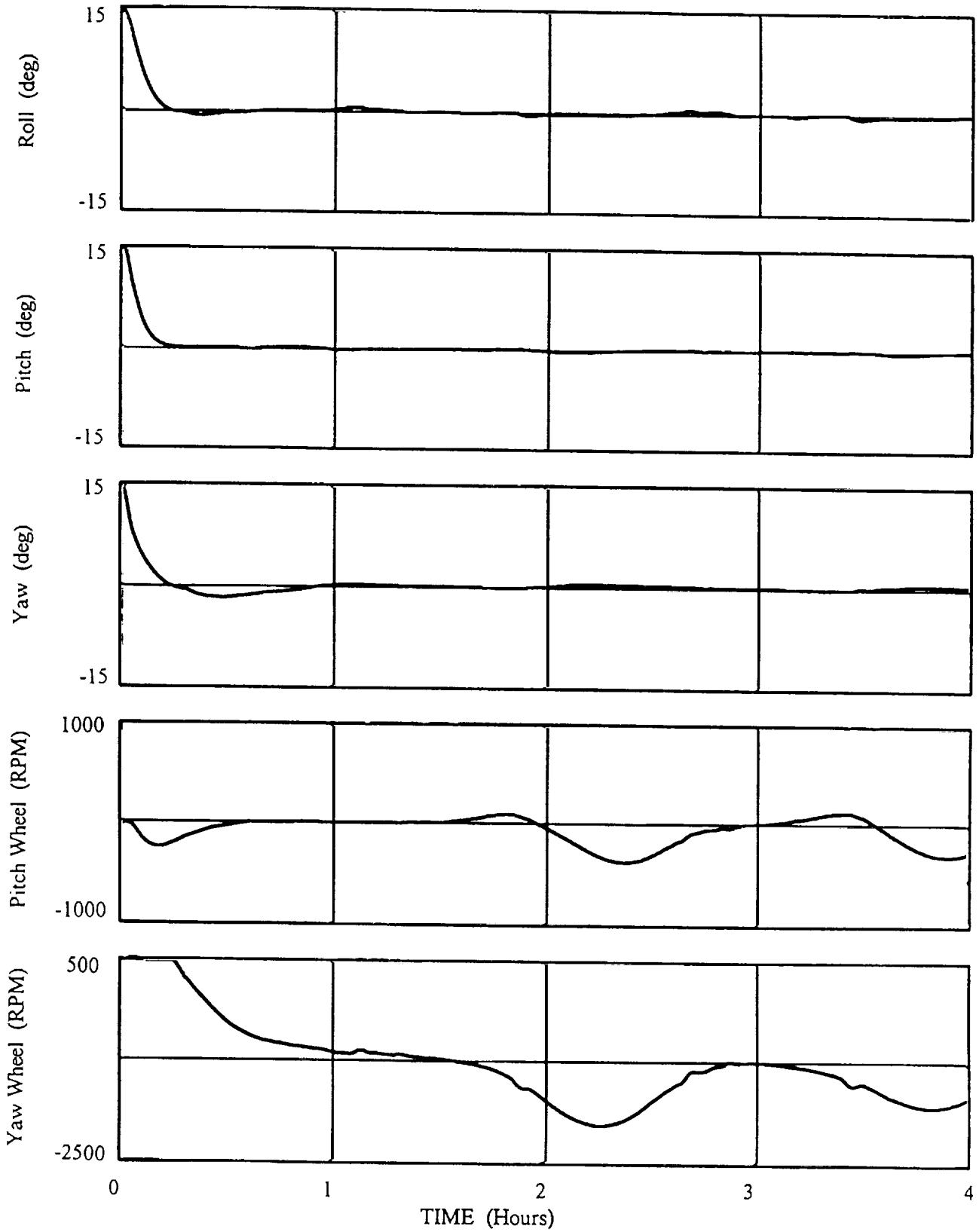
Simulation Series 2



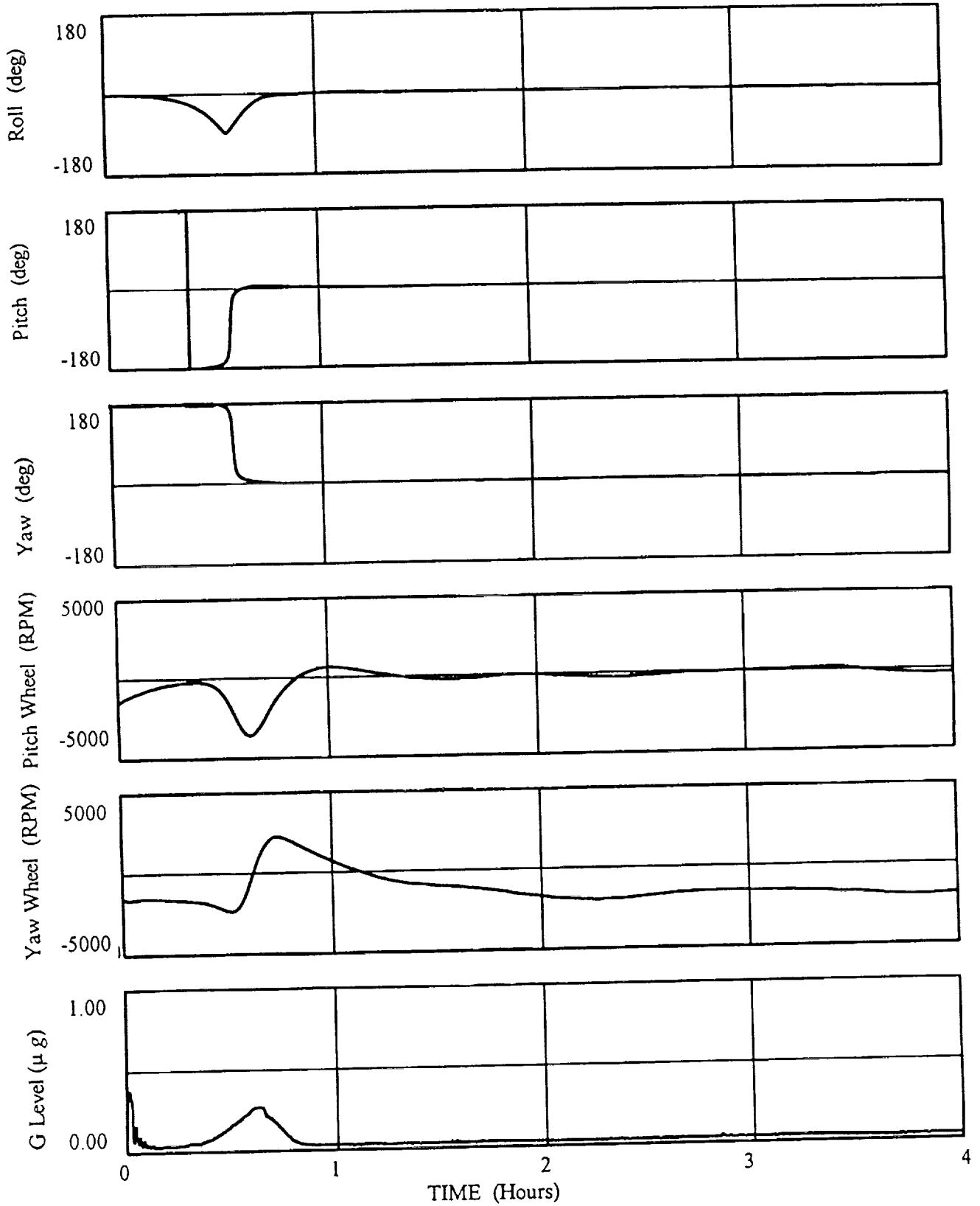
Simulation Series 3



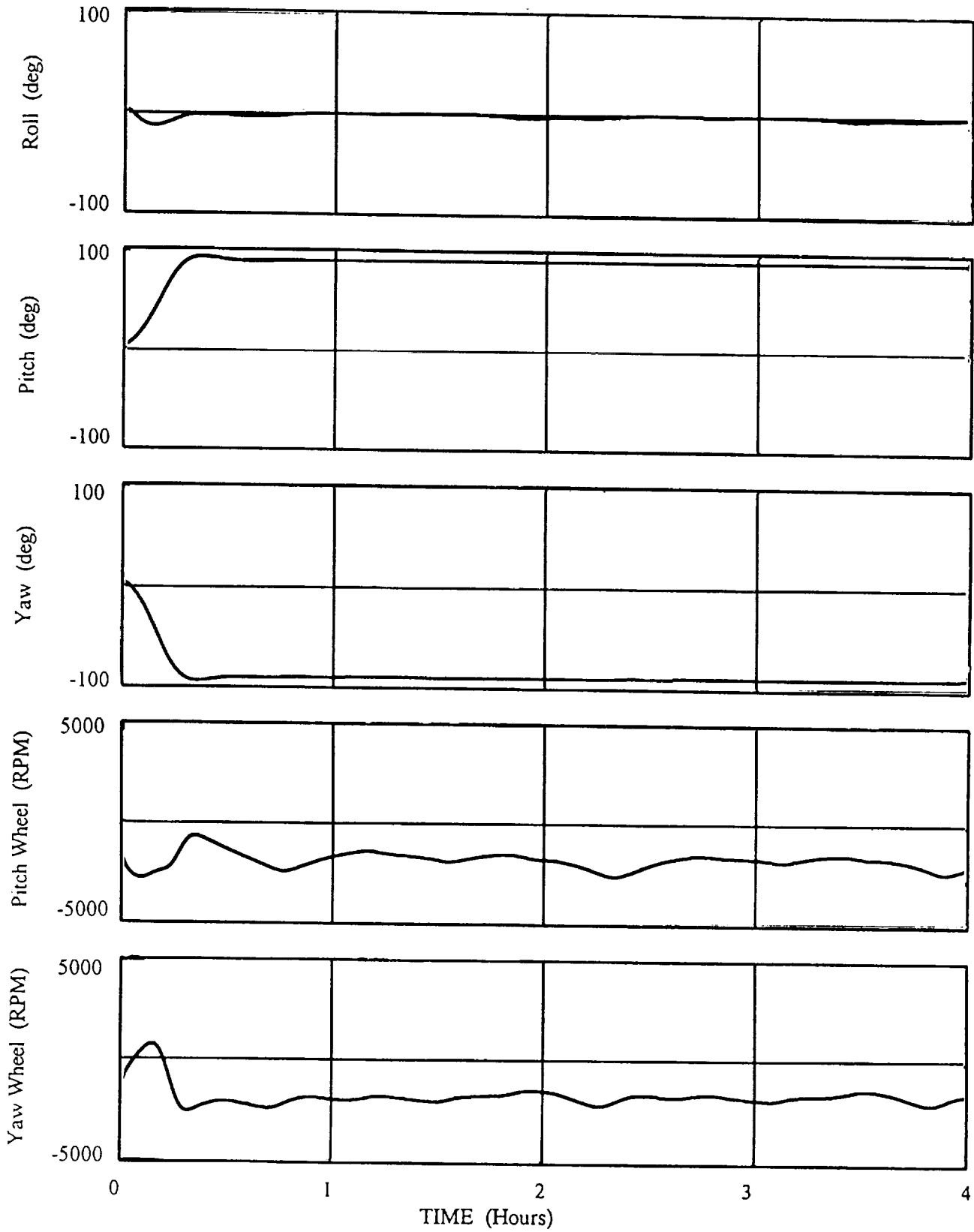
Simulation Series 4



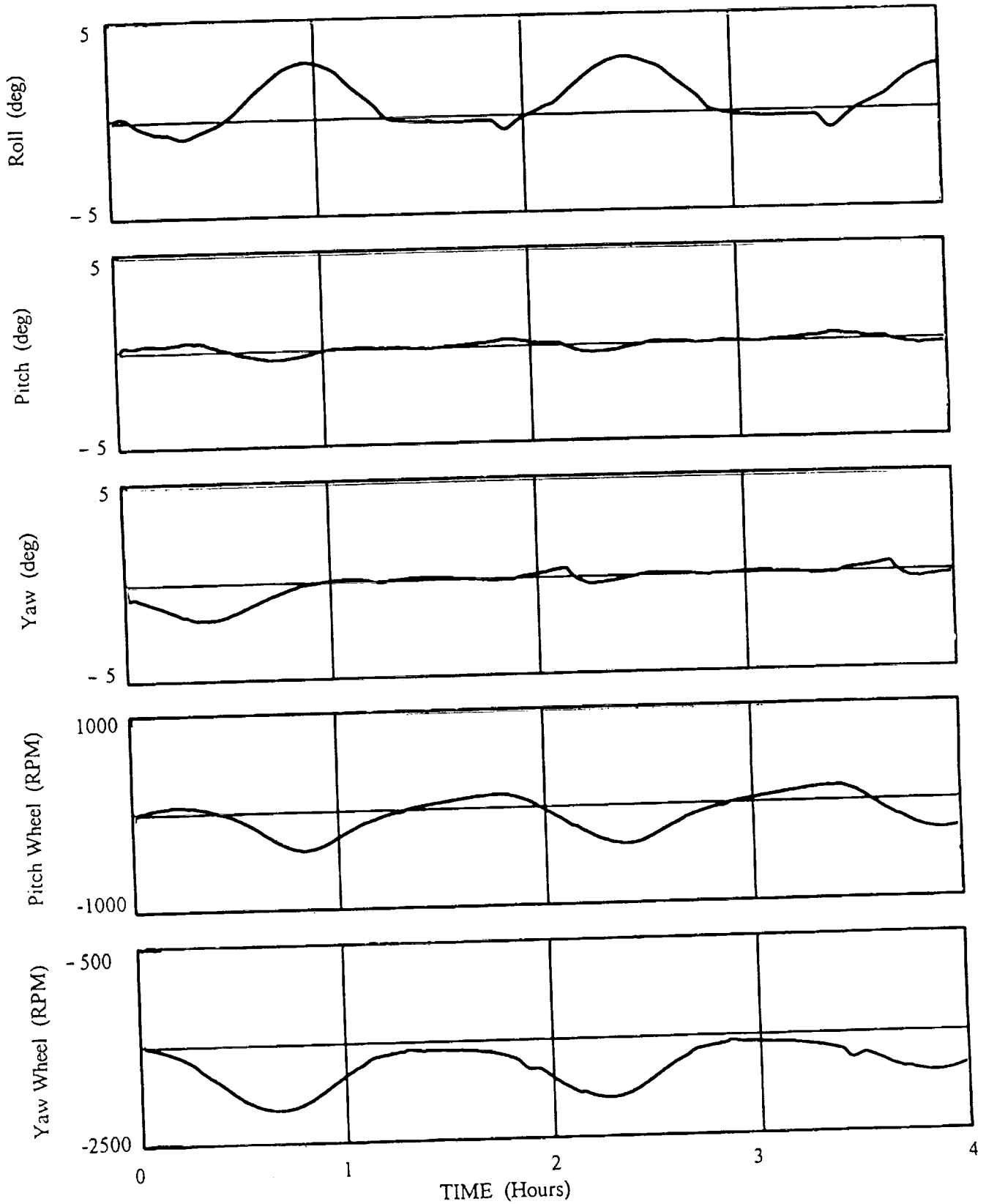
Simulation Series 5



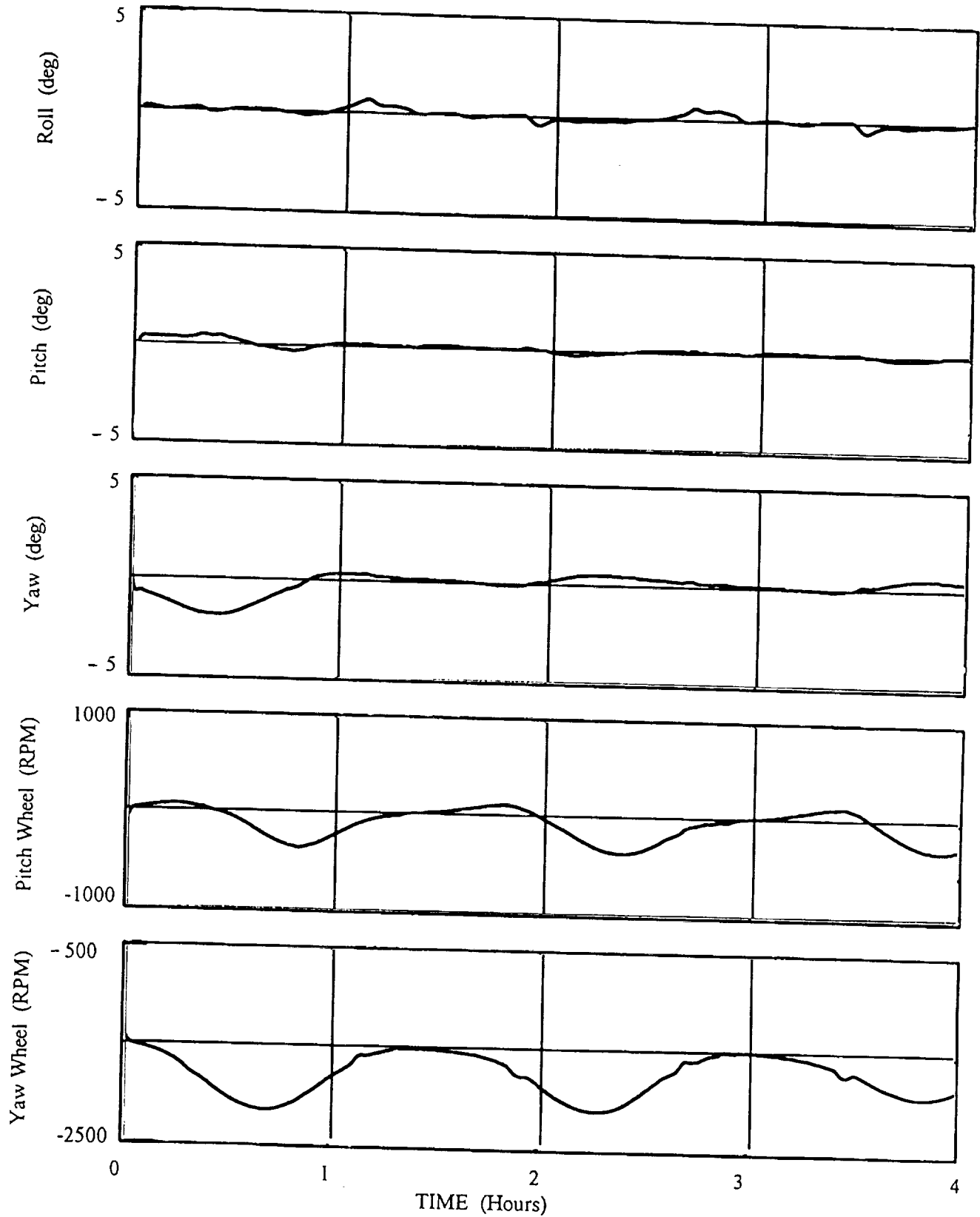
Simulation Series 6



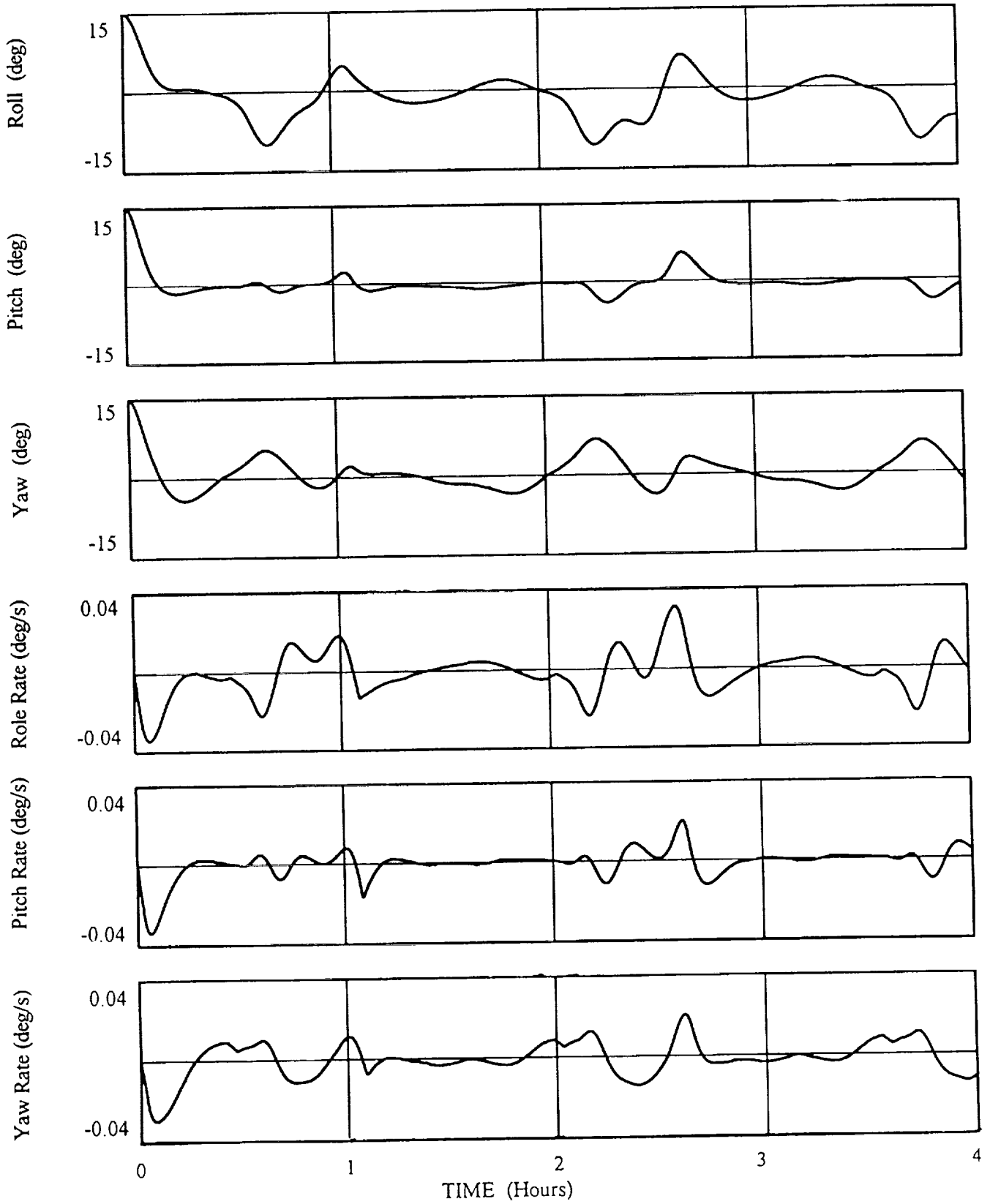
Simulation Series 7A



Simulation Series 7B



Simulation Series 8



FLIGHT MECHANICS/ESTIMATION THEORY SYMPOSIUM

MAY 17-19, 1994

SESSION 5

